

Substrate-Dependent Orientation and Polytype Control in SiC Nanowires Grown on 4H-SiC Substrates

Bharat Krishnan, Rooban Venkatesh K. G. Thirumalai, and Yaroslav Koshka*

Mississippi State University, Department of Electrical and Computer Engineering, Mississippi State, Mississippi 39762, United States

Siddarth Sundaresan

GeneSiC Semiconductor Inc., 43670 Trade Center Place, Suite 155, Dulles, Virginia 20166, United States

Igor Levin and Albert V. Davydov

National Institute of Standards and Technology, Gaithersburg, Maryland 20899, United States

J. Neil Merrett

Air Force Research Laboratory, Wright-Patterson Air Force Base, Ohio 45433, United States

Received October 20, 2010; Revised Manuscript Received December 8, 2010

ABSTRACT: SiC nanowires were grown on monocrystalline 4H-SiC wafers by chemical vapor deposition using the vapor–liquid–solid growth mode. The growth direction of the nanowires was dictated by the crystallographic orientation of the 4H-SiC substrates. Two distinct types of nanowires were obtained. The first type crystallized in the 3C polytype with the $\langle 111 \rangle$ nanowire axes. These nanowires grew at 20° with respect to the substrate c -planes and exhibited high densities of stacking faults on those $\{111\}$ planes that are parallel to the substrate c -planes. The second type featured the 4H structure albeit with a strong stacking disorder. The stacking faults in these nanowires were perpendicular to the $[0001]$ nanowire axes. Possible growth mechanisms that led to the formation of 3C and 4H polytypes are discussed.

Introduction

A wide band gap, large critical electric field, and high thermal conductivity make SiC uniquely suitable for high-power and high-temperature electronics applications,¹ while superior physical and chemical stability and biocompatibility make it very promising for biomedical, gas-sensing, and other applications in harsh environments.^{2–4} These advantages are expected to benefit devices utilizing SiC nanowires (NWs). The existence of different polytypes of SiC introduces additional flexibility; however, stabilizing a particular SiC polymorph during growth is a challenge.

Synthesis of SiC NWs predominantly relies on the vapor–liquid–solid (VLS) growth mode. The list of reported synthesis techniques includes reaction of carbon-source gases with Si substrates,⁵ pyrolysis of powders containing the source materials,^{6–8} reaction of source gases with carbon nanotubes,^{9,10} microwave heating-assisted physical vapor transport,¹¹ and chemical vapor deposition (CVD).^{12–14}

Various substrates have been used for SiC NW synthesis, including SiO₂,^{14–16} graphite,^{6,8,17,18} poly-SiC,¹² etc. Only a few attempts to utilize monocrystalline 6H⁷ and 4H^{11,19} SiC substrates have been reported. The use of monocrystalline SiC substrates offers a promise of polytype control in SiC NW growth.

SiC NWs commonly crystallize in the 3C polytype. Different crystallographic orientations of the 3C NW axis have been reported, including $\langle 111 \rangle$,^{5,12,17,14} $\langle 110 \rangle$, $\langle 100 \rangle$,¹³ and $\langle 112 \rangle$.^{11,13} Relatively rare observations of other polytypes include 6H,^{6–8,12,20} 2H,^{15,12} and 15R.^{12,18} Only a few studies have reported traces of the 4H polytype.^{18,21}

A successful attempt to utilize 6H-SiC substrates for achieving substrate-determined NW alignment was reported in ref 7. Evidence for the domination of the 6H polytype was provided.

No information exists about substrate-determined preferential orientations and the dominant polytypes of NWs grown on 4H SiC substrates. Yet, our ability to achieve specific SiC polytypes is critical for controlling electrical properties of SiC NWs, while the control of the growth orientation (e.g., alignment of the NWs along the particular direction) may facilitate formation of desirable device structures. In this work, alignment and polytype control of SiC NWs grown on commercial 4H-SiC substrates by CVD is investigated.

Experimental Section

Growth of SiC NWs using the vapor–liquid–solid (VLS) mode was conducted in a hot-wall CVD reactor at 150 Torr with H₂ as the carrier gas, and SiCl₄ and CH₃Cl as the silicon and carbon source, respectively. Heavily doped n-type 4H-SiC (0001) substrates vicinally cut 8° toward the $[1\bar{1}20]$ direction were used, which are standard for achieving polytype reproducibility via the step-flow growth mechanism in SiC epitaxy.²² Blanket as well as patterned Au, Ni, or NiSi catalyst layers were deposited on the samples by physical vapor

*To whom correspondence should be addressed. E-mail: ykoshka@ece.msstate.edu.

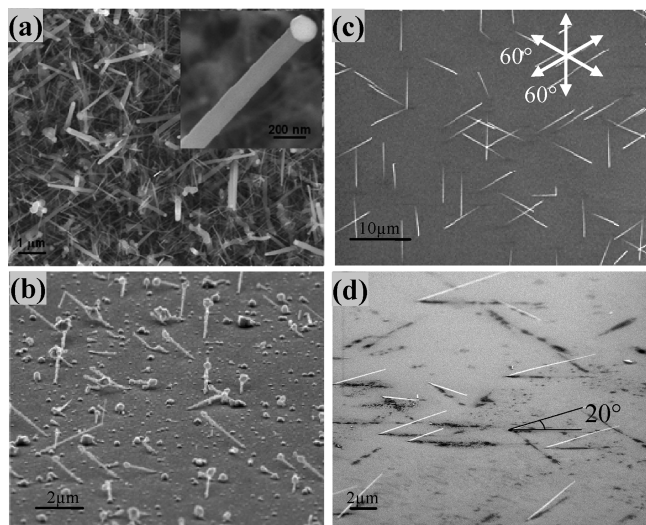


Figure 1. (a) A tilted view of dense SiC NW array grown using Ni catalyst at 1150 °C, (b) a tilted view of sparse NWs grown using Au catalyst at 1100 °C, (c, d) the top and tilted views of sparse NWs grown using NiSi catalyst at 1150 °C.

deposition from the gold, nickel, and silicon-nickel alloy of 1:1 composition, respectively. The NWs were characterized by Nomarski optical microscopy, scanning electron microscopy (SEM), X-ray diffraction (XRD), and electron diffraction and imaging in a transmission electron microscope.

Results and Discussion

The most favorable temperature ranges for SiC NW growth varied somewhat among the three different catalysts used.¹⁹ For a typical catalyst thickness of 5 nm, the optimal growth temperatures were 1150 °C (Figure 1a) and 1100 °C (Figure 1b) for Ni and Au, respectively. A very high density of NWs on the surface was obtained using Ni, which was very different from the relatively sparse NWs grown with Au catalyst (Figure 1b). The NW density is also sensitive to the thickness of the catalyst layer, pregrowth heat-treatment conditions, etc., but a discussion of these factors is beyond the scope of this paper.

The use of the NiSi catalyst at the same growth temperature of 1150 °C as selected for the Ni-based growth provided NWs thicknesses and lengths comparable to those obtained with Ni. However, NiSi-assisted growth yielded significantly lower densities of NW per unit area of the substrate (Figure 1c,d), which facilitated the identification of the preferential NW growth directions.

As seen in the top-view SEM images (e.g., Figure 1c), NWs grew along the six directions at the azimuth angles of 60° with respect to each other. The NW axes were oriented at 20° with respect to the basal plane (*c*-plane) of the 4H-SiC substrate (i.e., 70° to the *c*-axis of the substrate), taking into account the 8° miscut of the substrate surface. A certain fraction of nearly vertical NWs were also observed in the samples having a high density of NWs.

The XRD pattern from the NWs grown at 1150 °C using Ni catalyst is shown in Figure 2. XRD revealed SiC reflections that were absent in the analogous patterns measured from the bare substrates.

The main SiC lines in Figure 2 could be assigned to the cubic 3C and/or hexagonal (i.e., 4H) polytypes. However, the sidebands that flank the 111 reflection match the 4H-SiC polytype,

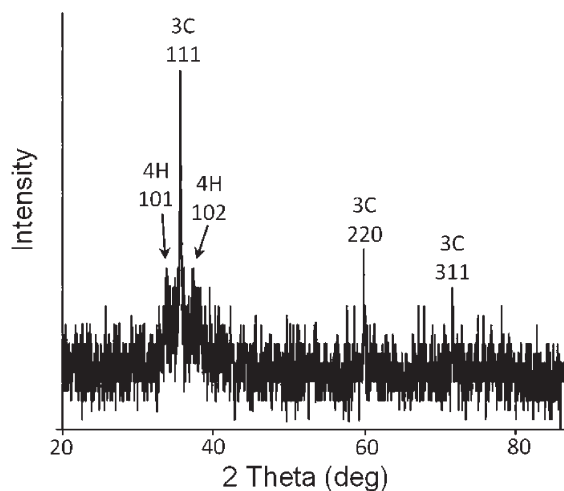


Figure 2. XRD pattern from dense SiC NW array grown on 4H-SiC substrate at 1150 °C. The reflections 111, 220, and 311 are indexed according to the 3C polytype. The peaks flanking the 111 reflection match the 4H polytype.

even though the measurements were too noisy to make a reliable identification.

Qualitatively similar XRD patterns were observed when measuring different samples grown with different catalysts and also at a few different growth temperatures. More detailed comparison of different catalysts is beyond the scope of this work.

Higher-magnification SEM as well as energy dispersive X-ray (EDX) analysis during transmission electron microscopy (TEM) measurements revealed the presence of metal droplets at the NW tips, which confirmed that the NW growth occurs following the VLS mode.

Selected area electron diffraction (SAED) patterns and bright/dark field images were collected for the NWs from the Ni-based sample. Two main types of NWs were observed (Figure 3), which hereafter will be referred to as Type A and Type B. Both types exhibit high densities of stacking faults (SF) as reflected in the nearly continuous rods of diffuse intensity in the SAED patterns.

In Type A, the fault planes are orthogonal to the NW axis and the electron diffraction (ED) patterns exhibit discernible maxima at $1/4d^*$ indicated using arrows in Figure 3a, where d^* is a reciprocal of the *c*-layer spacing for hexagonal SiC. These results confirm the presence of the 4H polytype with a strong stacking disorder consistent with the XRD patterns.²³ The NW axis in Type A is parallel to the [0001] direction.

In contrast, the SF planes in Type B are aligned at 70° to the NW axis (Figure 3b). These NWs exhibit the 3C structure with the NW axis parallel to the [111] direction.

It should be noted that the Type-B alignment of SFs was dominating also in other samples, including the samples produced with NiSi and Au catalysts. While it was expected that the catalyst composition and growth temperature should also influence the growth direction of the NWs, no such effect was observed in this study.

The actual angle between the axis of Type-A NWs and the substrate remains uncertain. An intuitive argument for NWs with their axis parallel to the [0001] direction to reproduce the polytype of the substrate would require a vertical growth direction (offset by the 8° orientation of the substrate surface with respect to the *c*-plane). Indeed, such nearly vertical NWs were observed in the SEM images of the Ni-based samples;

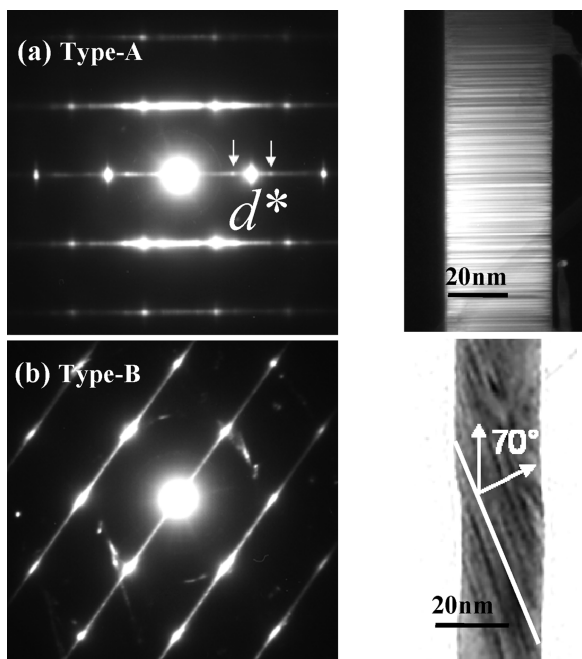


Figure 3. SAED of (a) Type-A NW having the fault planes orthogonal to the NW axis and (b) Type-B NW with the growth axis at 70° to the $[0001]$ direction of the substrate. SAED in (a) reveals the 4H polytype with a strong stacking disorder as manifested in superlattice reflections at $1/4d^*$ indicated with arrows. SAED in (b) displays a 3C NW with a high density of $\{111\}$ stacking faults.

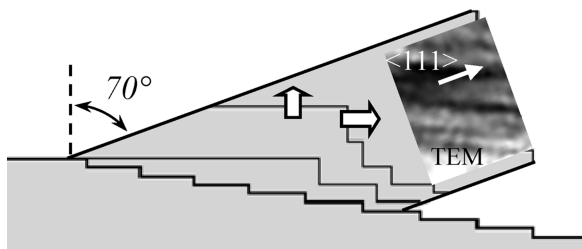


Figure 4. Schematic illustration of the growth process for a NW growing at 70° with respect to the c -axis of the substrate. The inset shows the TEM image of a 3C NW with SF parallel to the basal plane of the substrate.

however, establishing crystallographic orientation of these NW proved difficult because of high densities of NW on the substrates.

Growth of the Type-B 3C NWs shown in Figure 3 appears to be strongly influenced by the 4H-SiC substrate. The 20° angle between the NW and the c -plane of the substrate in Figure 1, combined with the $\langle 111 \rangle$ orientation of the NW axis (Figure 3b), suggests the growth mechanism schematically illustrated in Figure 4. The $\langle 111 \rangle$ -oriented 3C NWs grow on the (0001) surface of the 4H-SiC substrates at 70° to the c -axis of the substrate, so that one set of the NW $\{111\}$ planes oriented at 70° to the NW axis is parallel to the c -planes of the substrate.

It should be noted that the 70° angle (i.e., 20° angle to the (0001) surface) is the same as previously reported for NWs grown on 6H-SiC substrate in ref 7. In 6H-SiC, the 20° angle corresponds to $\bar{1}102$ directions in the substrate; however, in 4H-SiC, this angle does not correspond to any of the low-index directions. We speculate that the 70° angle in 6H-SiC⁷ could favor both the 6H NW growth along the $[\bar{1}102]$

direction (70.56° to the c -axis) and the 3C NW growth along the $[111]$ direction; in both cases, the SF planes in the NW occur parallel to the (0001) substrate surface.

For 4H-SiC substrates, the growth of 4H NWs along the $[\bar{1}102]$ direction would require a $\sim 60^\circ$ (rather than 70°) angle to the c -plane of the substrate. The 3C growth with $[111]$ NW axis dictates the 70° angle so that the $(\bar{1}11)$ plane (i.e., the SF plane) is parallel to the basal plane of the substrate. Apparently, this orientation relationship yields the best lattice matching between 3C NWs and the 4H substrate. The relevant d -spacings in the (0001) plane of 4H-SiC ($a = 3.080 \text{ \AA}$) are $d_1 = 1.54 \text{ \AA}$ and $d_2 = 2.67 \text{ \AA}$ for the $(11\bar{2}0)$ and $(1\bar{1}00)$ planes, respectively. The (110) and (112) d -spacing values for 3C SiC ($a = 4.349 \text{ \AA}$) are 3.075 \AA and 1.775 \AA , respectively.

This discussion does not explain why the 3C polytype in the NWs forms at all. As illustrated in Figure 4, the 8° off-axis (0001) surface of the 4H-SiC substrate provides a sufficient number of steps, which normally ensures reliable polytype reproduction in the regular homoepitaxial growth of SiC, even at growth temperatures below 1300°C .²⁴ However, random nucleation of the 3C polytype has been long known to occur if the growth temperature is not high enough or the precursor supersaturation is too high, both suppressing the adatom mobility at the surface.²²

In the VLS growth, the temperatures are much lower while the effective supersaturation of the growth precursors in the catalyst layer at the growth surface is much higher than that at the bare surface in the homoepitaxial vapor–solid (VS) growth, which is manifested by the much higher growth rates of the NWs ($> 40 \mu\text{m/h}$ in the experiments at 1150°C) compared to $5\text{--}6 \mu\text{m/h}$ in our regular low-temperature VS growth of SiC epilayers using the same growth precursors.²⁴ Furthermore, an equivalent of the surface mobility in regular epitaxial growth (and therefore the propensity of the random nucleation at the expense of the step-flow growth) is unknown for the VLS growth of SiC. All these factors mean that the step-flow mechanism for reliable polytype reproduction may not be as easily sustained during NW growth. Yet, the dominance of the 4H polytype in Figure 3a indicates that it can be achieved.

A vertical growth direction is expected to be not the only one favoring the 4H-SiC polytype. The $[\bar{1}102]$ growth direction was identified in ref 7 as favorable for 6H-SiC NWs. This direction is likely to be favorable also for 4H; however, it will result in a 30° orientation of the 4H-SiC NWs with respect to the (0001) substrate surface. Future work will be focused on identifying conditions favoring both vertical and 30° orientations that are expected to dominate for the 4H polytype in SiC NW growth.

Conclusion

In summary, epitaxial growth of SiC NWs on (0001) surfaces of 4H-SiC substrates was investigated. Nanowires of both 4H and 3C polytypes were obtained. The NWs grew on 4H-SiC substrates epitaxially, with the growth direction determined by the substrate. The 4H-SiC NWs had axes parallel to the $[0001]$ direction. The $\langle 111 \rangle$ axes of the 3C-SiC NWs were oriented along the six directions at the azimuth angles of 60° with respect to each other and 20° with respect to the c -plane of the 4H-SiC substrate. Use of 4H-SiC surfaces having crystallographic orientations other than (0001) employed in this work is expected to enable growth of highly aligned SiC nanowires. The growth conditions favoring nanowires of 4H-SiC polytype are yet to be established.

References

- (1) Palmour, J. W. *Mater. Sci. Forum* **2006**, 527–529, 1129.
- (2) Li, X.; Wang, X.; Bondokov, R.; Morris, J.; An, Y. H.; Sudarshan, T. InterScience Wiley: New York, **2004**; pp 353–360.
- (3) Yakimova, R.; Pectoral, R. M., Jr.; Yazdi, G. R.; Vahlberg, C.; Lloyd Spetz, A.; Uvdal, K. *J. Phys. D: Appl. Phys.* **2007**, 40, 6435–6442.
- (4) Neudeck, P. G.; Spry, D. J.; Trunek, A. J.; Evans, L. J.; Chen, L.-Y.; Hunter, G. W.; Androjna, D. *Mater. Sci. Forum V.* **2009**, 600–603, 1199–1202.
- (5) Kim, H. Y.; Park, J.; Yang, H. *Chem. Commun* **2003**, 256–257.
- (6) Wang, H.; Xie, Z.; Yang, W.; Fang, J.; An, L. *Cryst. Growth Des.* **2008**, 8 (11), 3893–3896.
- (7) Wang, H.; Lin, L.; Yang, W.; Xie, Z.; An, L. *J. Phys. Chem. C* **2010**, 114, 2591–2594.
- (8) Gao, F.; Yang, W.; Wang, H.; Fan, Y.; Xie, Z.; An, L. *Cryst. Growth Des.* **2008**, 8 (5), 1461–1464.
- (9) Pan, Z. W.; Lai, H. L.; Au, C. K.; Duan, X. F.; Zhou, W. Y.; Shi, W. S.; Wang, N.; Lee, C. S.; Wong, N. B.; Lee, S. T.; Xie, S. S. *Adv. Mater.* **2000**, 12, 1186–1190.
- (10) Wallis, K. L.; Weiligor, M.; Zerda, T. W.; Stelmakh, S.; Gierlotka, S.; Palosz, B. *J. Nanosci. Nanotechnol.* **2008**, 8, 3504–3510.
- (11) Sundaresan, S. G.; Davydov, A. V.; Vaudin, M. D.; Levin, I.; Maslar, J. E.; Tian, Y. L.; Rao, M. V. *Chem. Mater.* **2007**, 19 (23), 5531–5537.
- (12) Pampuch, R.; Górny, G.; Stobierski, L. *Glass Phys. Chem.* **2005**, 31 (3), 370–376.
- (13) Peng, H. Y.; Zhou, X. T.; Lai, H. L.; Wang, N.; Lee, S. T. *J. Mater. Res.* **2000**, 15 (9), 2020–2026.
- (14) Seong, H. K.; Park, T. E.; Lee, S.; Lee, K. R.; Park, J. K.; Choi, H. J. *Met. Mater. Int.* **2009**, 15 (1), 107–111.
- (15) Yao, Y.; Lee, S. T.; Li, F. H. *Chem. Phys. Lett.* **2003**, 381, 628–633.
- (16) Seong, H. K.; Choi, H. J.; Lee, S. K.; Lee, J. I.; Choi, D. J. *Appl. Phys. Lett.* **2004**, 85 (7), 1256–1258.
- (17) Wu, R.; Li, B.; Gao, M.; Chen, J.; Zhu, Q.; Pan, Y. *Nanotechnology* **2008**, 19, 335602.
- (18) Bechelany, M.; Brioude, A.; Cornu, D.; Ferro, G.; Miele, P. *Adv. Funct. Mater.* **2007**, 17, 939–943.
- (19) Kotamraju, S.; Krishnan, B.; Koshka, Y.; Sundaresan, S.; Issa, H.; Singh, R. *Mater. Res. Soc. Symp. Proc.* **2009**, 1178E, 1178-AA03–06.
- (20) Wei, G.; Qin, W.; Wang, G.; Sun, J.; Lin, J.; Kim, R.; Zhang, D.; Zheng, K. *J. Phys. D: Appl. Phys.* **2008**, 41, 235102.
- (21) Yoshida, H.; Kohno, H.; Ichikawa, S.; Akita, T.; Takeda, S. *Mater. Lett.* **2007**, 61, 3134–3137.
- (22) Kimoto, T.; Matsunami, H. *J. Appl. Phys.* **1995**, 78, 3132.
- (23) Koumoto, K.; Takeda, S.; Pai, C. H.; Sato, T.; Yanagida, H. *J. Am. Ceram. Soc.* **1989**, 72, 1985.
- (24) Kotamraju, S.; Krishnan, B.; Koshka, Y. *Phys. Status Solidi RRL* **2009**, 3 (5), 157.